International Journal of Engineering Trends and Technology
ISSN: 2231–5381 / https://doi.org/10.14445/22315381/IJETT-V72I8P131

Volume 72 Issue 8, 332-341, August 2024

Original Article

Improved Spider Monkey Optimization with Deep Learning Model for Tomato Leaf Disease Recognition

K. Sundaramoorthi[1], Mari Kamarasan[2]

[1,2]*Department of Computer and Information Science, Annamalai University, Tamil Nadu, India.*

[1]*Corresponding Author : csksundar7@gmail.com*

Received: 26 February 2024 Revised: 18 June 2024 Accepted: 02 July 2024 Published: 28 August 2024

Abstract *- Tomato plant leaf disease recognition is a crucial feature of smart farming, as it allows early analysis and intervention to avoid the spread of diseases that devastate tomato crops. With the advent of Machine Learning (ML), automated disease recognition methods have become increasingly popular. This method involves gathering a database of images of either healthy or diseased tomato leaves. Image processing systems are then utilized to enhance and preprocess these images. Deep learning (ML) models, mostly Convolutional Neural Networks (CNNs), are trained on this database to classify leaves as diseased or healthy depending on their visual characteristics. These methods offer quick and consistent assessments of leaf health. Therefore, this study proposes an enhanced spider monkey optimization with a DL model for tomato leaf disease recognition (ISMODL-TLDR) technique. The ISMODL-TLDR technique incorporates the DL models with a hyperparameter tuning model for tomato leaf disease recognition. Wiener filtering (WF) is initially used as a preprocessing stage to improve the leaf image quality and reduce noise. Besides, an EfficientNet model captures intricate patterns from the preprocessed images. To fine-tune the model's hyperparameters effectively, an improved spider monkey optimization (ISMO) model can be introduced, which intelligently tunes the hyperparameters. At last, the classification stage employs long short-term memory (LSTM), enabling the method to comprehend temporal reliabilities in leaf disease progression. The simulation analysis portrays the enhanced achievement of the ISMODL-TLDR technique in terms of classification accuracy. The ISMODL-TLDR technique holds great promise for sustainable agriculture practices, helping farmers make informed decisions and mitigate disease-related crop losses.*

Keywords *- Crop disease detection, Metaheuristics, Computer vision, Deep learning, Hyperparameter.*

1. Introduction

The development of agriculture is closely related to the innovation of science, computer technology, and Artificial Intelligence (AI), which can be developed as a sustainable approach for improving agricultural efficiency by providing beneficial guidance and suggestions about crops [1]. Moreover, vegetables or crops have been primarily employed in countries all over the world and encounter the requirements in several methods [2]. Tomato (SolanumLycopersicum L.) is the most frequent, another significant vegetable or fruit crop, compared to potato (Solanumtuberosum L.). Tomatoes are globally liked as a sauce, vegetable, natural skin care product, and salad [3]. However, numerous tomato leaf diseases prominently decrease the tomato fruit and occasionally destroy the plant [4]. These diseases are identified by employing technology or manually, and they have the potential to reproduce the tomato yield and satisfy the requirements of making the world [5]. Plant diseases are an essential issue in farming, resulting in significant crop losses and financial implications [6]. Early and precise plant disease recognition is crucial for efficiently controlling the disease and viable crop production. Fast and early detection of plant diseases could be supported by preventative actions and avoiding the widespread spread of diseases [7]. Standard analytic techniques, namely manual chemical testing and visual inspection, have been higher-cost, laborious, and time-consuming. With the development of computer technology, image-based plant disease identification provided the benefits of being rapid, resource-efficient, and cost-effective [8]. Research workers have developed and utilized Several image identification techniques for plant disease detection, including support vector machine (SVM), artificial bee colony (ABC), and other ML techniques. Recently, DL methods have represented optimistic outcomes in plant leaf disease detection [9]. However, Researcher workers can make a series of enhancements to DL methods because of the various signs, challenging environment, and random distribution of plant leaf disease images. Research workers developed a new plant leaf disease detection technique that depends upon a deep CNN (DCNN), which can attain improved identification outcomes by establishing suitable convolutional layers [10]. This study proposes an enhanced spider monkey optimization with a DL model for tomato leaf disease recognition (ISMODL-TLDR) technique.

The presented ISMODL-TLDR technique incorporates the DL models with a hyperparameter tuning model for tomato leaf disease recognition. Wiener filtering (WF) is initially used as a preprocessing stage to improve the leaf image quality and reduce noise. Besides, an EfficientNet model captures intricate patterns from the preprocessed images. To fine-tune the model's hyperparameters effectively, an improved spider monkey optimization (ISMO) model can be introduced, which intelligently tunes the hyperparameters. At last, the classification stage employs long short-term memory (LSTM), enabling the method to comprehend temporal reliabilities in leaf disease progression. The simulation analysis portrays the enhanced achievement of the ISMODL-TLDR technique in terms of classification accuracy.

2. Related Works

In [11], a DL-assisted model implementing the conditional Generative Adversarial Network (GAN) namely C-GAN model is proposed. Subsequently, a DenseNet_121 approach is given training on real and synthetic imageries by employing TL for classification. Roy et al. [12] introduced a study emphasizing a well-developed new approach by the Deep Neural Networks (DNN) model. This developed new architecture was employed by incorporating standard ML techniques Principal Component Analysis (PCA) and modified DNN techniques termed PCA DeepNet. The hybridized model also contains GAN to acquire a better combination of databases. An identification was performed by employing the faster region-based CNN (F-RCNN) technique.

The authors [13] proposed a hybrid framework. The TL and fine-tuning approaches enhance the effectiveness of various pre-trained methods. Two techniques are chosen to design the hybrid approach. In [14], a reconstructed Residual Dense Network (RDN) is developed; this hybrid DL approach integrates the benefits of deep-ResNet and DenseNet models. The original RDN approach is initially employed in image super-resolution. Therefore, it is necessary to reconstruct the network architecture to classify tasks by adapting input image features and hyperparameters. Guerrero-Ibañez and Reyes-Muñoz [15] implemented a technique that depends on the CNN model. To prevent overfitting, GANs are exploited. In [16], 2 CNN-assisted methods such as GoogLeNet and VGG16 are implemented.

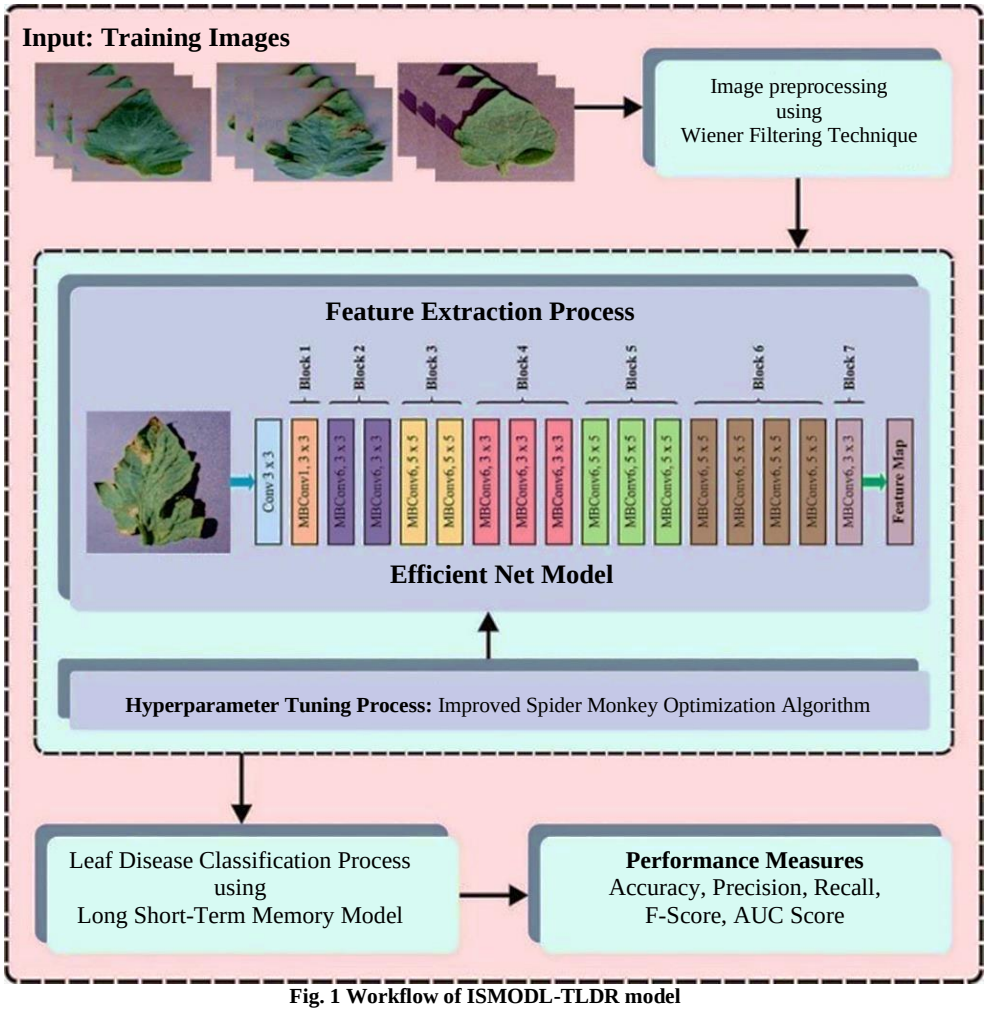

Fig. 1 Workflow of ISMODL-TLDR model

Anandhakrishnan and Jaisakthi [17] introduced the DCNN method. The authors developed an automated process to detect tomato leaf disease utilizing DCNN. Mahadevan, Punitha, and Suresh [18] propose a Deep Spectral GAN ($DSGAN^2$) method. This approach used Improved Threshold Neural Network (ITNN), Segment Multiscale Neural Slicing (SMNS), and Spectral Scaled Absolute FS (S^2AFS) techniques for image enhancement, segmentation, and optimum feature selection. In [19], the Enhanced Gray Wolf Optimizer (EGWO) model is presented. Kaushik et al. [20] introduce a depth-wise separable-based adaptive DNN (DSDNN) model. This method comprises Gaussian filtering and Enthalpy-based graph clustering techniques for preprocessing and segmentation.

3. The Proposed Model

This paper proposes an automated tomato leaf disease detection and classification approach called the ISMODL-TLDR technique. The presented ISMODL-TLDR technique incorporates DL models with hyperparameter tuning for tomato leaf disease recognition. It involves processes namely pre-processing, extraction, tuning, and classification using WF, EfficientNet, ISMO, and LSTM. Figure 1 depicts the workflow of the ISMODL-TLDR technique.

3.1. WF-based Preprocessing

The WF model is employed to eliminate noise in images. WF is a primary method in image processing deployed to enhance the quality of digital photos by decreasing noise and recovering valuable image details [21]. By employing either the image's power spectrum or evaluated noise power spectrum, WF fine-tunes dynamically for every pixel from the image, executing suitable filters for amplifying signal modules but attenuating noise. Figure 2 shows the sample and resultant images after applying WF. The WF is stated as:

$$G(u,v) = H(u,v)F(u,v) + \eta(u,v)$$

Where $G(u,v)$ is the output image after applied to the above equation, $H(u,v)$ is the degradation function, $F(u,v)$ is an image in the frequency domain, and $\eta(u,v)$ is the noise function in the frequency domain. This adaptive system makes WF mostly effective when noise levels differ across an image, contributing to better image clarity and supporting tasks like image restoration, deblurring, and noise reduction.

Original image After noise removal

Fig. 2 Sample image and resultant image after applying WF

Generally, WF preserves the significant image features and reduces the noises presented in the image using optimal Mean Square Error (MSE).

3.2. EfficientNet Feature Extractor

At this stage, the EfficientNet model extracts the features. Tan et al. [22] designed to establish a model scaling process which optimizes either speed or accuracy. To accomplish this, re-examined many sizes of model scaling presented by its ancestors comprising network width, depth, and image resolution. However, earlier research concentrated on increasing one of the sizes to enhance accuracy; the authors detected that these sizes could be jointly influential and presented EfficientNet. In detail, an initial definition of the problem was initially used to find the connection between network width, depth, and image resolution in accomplishing an accuracy technique. It is considered that the whole net is N, and the i^{th} layer can be written as $Y_i = F_i(X_i)$, whereas $F_i$re presents the operator, $Y_i$denotes the resultant tensor, and X_j refers to the input tensor. Assume$N$comprises of k convolution layers, afterwards it is written as $N = F_k \odot \ldots \odot F_2 \odot F_1(X_1) = \odot_{j=1\ldots,k} F_j(X_j)$. Convolution layers can generally separate as similar structure phases; therefore, N is formulated as:

$$N = \odot_{1\ldots s} \ldots F_i^{L_i}(X\langle H_{j'}, W_{i'}, C_j\rangle) \quad (1)$$

Whereas i denotes the indexing phase, and $F_i^{L_i}$ refers to the convolution layer of i^{th}phase, F_i reiterates L_i times, and $\langle H_i, W_j, C_j\rangle$ implies the image's input shape. To mitigate the search space, particular restrictions are represented, which include fixing the basic network design, imposing equivalent scaling on every layer, and combining memory and calculation limitations. Therefore, the network scaling is only optimizer by multiplying the baseline network determined by $\hat{F}_i, \hat{L_i}, \hat{H}_i, \hat{W}_i, \hat{C}_i$ Equation 2 with constant enhancement:

$$\max Accuracy(N(d,w,r))$$
$$s.t. N(d,w,r) = \odot_{i=1\ldots s} \hat{F}_i^{\hat{L_i}}\left(X\langle r\times\hat{H}r\times\hat{W}, r\times C_i\rangle\right) \quad (2)$$
$$Memory\ (N) \le target\_memory$$
$$FLOPS(N) \le target\_flops$$

Whereas d, w, r denotes the co-efficient for scaling network width, depth, and resolution.

Afterwards, research conducted fine-tuning 1D at a time, while concurrently altering the overall three dimensions collectively. Here, a multi-scaling approach is represented. This approach utilizes several co-efficient ϕ for unvaryingly scaling the networking depth, width, and resolution:

$$depth: d = \alpha^{\phi}$$
$$width: w = \beta^{\phi} \quad (3)$$

$depth: r = \gamma^{\phi}$
$s.t. \alpha \cdot \beta^2 \cdot \gamma^2 \approx 2$, *where* $\alpha, \beta, \gamma \ge 1$ and denotes the fixed values represented by a small grid search.

The model assumed that doubling the network depth doubles FLOPS, while doubling the network resolution or width quadruples FLOPS, maintaining a regular function relative to $d, w2,$ and $r2$. Therefore, CNN scaling with Equation (3) enhances the entire FLOPS by $(\alpha \cdot \beta^2 \cdot \gamma^2)^{\phi}$. To maintain the FLOPS as a whole, enhance for around 2^{ϕ}, it is constrained $\alpha \cdot \beta^2 \cdot \gamma^2 \approx 2$.

3.3. Hyperparameter Optimization Process

To enhance the achievement of the Efficient Net technique, the ISMO method is incorporated to analyze the model's parameters, which acts as a significant part in the quick model convergence. The SMO is an SI optimization technique that emulates spider monkeys' merging and splitting behaviours while foraging [23]. The mutation and crossover operations segment the SMO technique from the Genetic Algorithm (GA). Moreover, the contribution value technique is used to decide the local and global leaders.

The contribution value method and hyper-volume performance indicator are used in this study to decide global and local leaders. As the contribution values of the outcome set rises, the output becomes better suited to its dispersion, leading to a greater area of independent superiority for the solution set. In the following, specific phases are given: Normalization of the target value; Pareto solution is organized orderly; Using the Equation(4), the reference point $z^*(z_1^*, z_2^*)$, z_r^* denotes the reference point value and σ is attained by the assessment; Based on formula at the Pareto front end or the edge, the contribution value is computed.

$$z_r^* = f_r^{\max} + \sigma(f_r^{\max} - f_r^{\min}) \tag{4}$$

$$CV_A = (Z_1^* - f_1^A)(Z_2^* - f_2^A) - \left(Z_1^* - \max(f_1^A, f_1^B)\right)(Z_2^* - f_2^A) \tag{5}$$

In this study, the hierarchical encoding system is used. The initial layer comprises a dimensional matrix of $2{\times}N^P$: the first row depicts the N^P order quantity, and the next row displays their processing sequence. The second layer comprises a dimensional matrix of $4 \times N^{lot}$: the initial row indicates the processing sequence of each lot, and subsequent rows denote the machine sequence across all stages.

During the Global Leader Phase (GLP), members of all the groups will update the location by approaching the global leader. During the Local Leader Phase (LLP), every member would upgrade the status by approaching their local leader.

The three layers of cross operation are categorized as crossing the processing order through the two-point cross technique. Based on order sorting, lot sorting can be attained; for the assignment of $a\ lot$, the partly coordinated crossover technique, like the two-point cross technique, is employed for crossing all the processes in order.

Arbitrarily choose order c, and its lot coding order to reverse sequence processing. The two order batches c arbitrarily choose $[0\ or\ 1]$ for all the processes for the dispersion variation and the process machine encoding. If it is 1, the equivalent gene is replaced or remains the same.

Optimal fitness is a significant ISMO method. An encoded performance is utilized to construct an enhanced output for candidate efficiency. The accuracy outcome is the critical factor implemented to build an FF.

$$Fitness = \max(P) \tag{6}$$

$$P = \frac{TP}{TP + FP} \tag{7}$$

Where FP and TP portray the values of false and true positive.

3.4. LSTM-Based Classification

After obtaining the prominent features such as colour description, texture characteristics, and shape description, which were discussed previously, the disease classification process and the LSTM model are applied. The LSTM is a particular kind of RNN, which has every benefit of RNN but overcoming its vanishing gradient problem [24]. Because of its specific structure, LSTM is proficient in learning long-term reliabilities. The LSTM block comprises a memory cell rather than neurons that are assumed as a memory unit with layer c_z at time z. Besides the memory cell, three adaptive and multiplicative units manage the data flow from the block. These units comprise forget f_z, input i_z, and output gates o_z. Data is permitted to gain entry to the block or the rest of the networks by input and output gates, and the forget gate resets the memory cell layer. Figure 3 defines the LSTM structure. The LSTM defines whether features are maintained or forgotten once the learning task. Accordingly, the LSTM can execute tasks over long-time sequences and determine long-range features. The LSTM block is defined, and the hidden layer (HL) h_z is measured by the subsequent formulas:

$$f_z = \sigma_g\left(W_f x_z + U_f h_{z-1} + b_f\right) \tag{8}$$

$$\begin{gathered} i_z = \sigma_g(W_i x_z + U_i h_{z-1} + b_i) \\ \mathrm{o}_z = \sigma_g(W_{\mathrm{o}} x_z + U_{\mathrm{o}} h_{z-1} + b_{\mathrm{o}}) \\ c_z = f_z \circ c_{z-1} + \mathrm{i}_z \circ \tanh(W_c x_z + U_c h_{z-1} + b_c) \\ h_z = o_z \circ \tanh(c_z) \end{gathered}$$

Whereas, $\circ$ implies the Hadamard production; f_z, i_z, and o_z signify the forget, input, and output gates, correspondingly; $W_o, U_o, U_f, W_f, U_i, W_i, W_c$, and U_c define the weighted matrices; b_f, b_i, b_0, and b_c represents the bias vectors; h_{z-1} indicates the outcome of LSTM at the preceding time $z-1$;x_z denotes the existing input; $\sigma()$ stands for the sigmoid activation function.

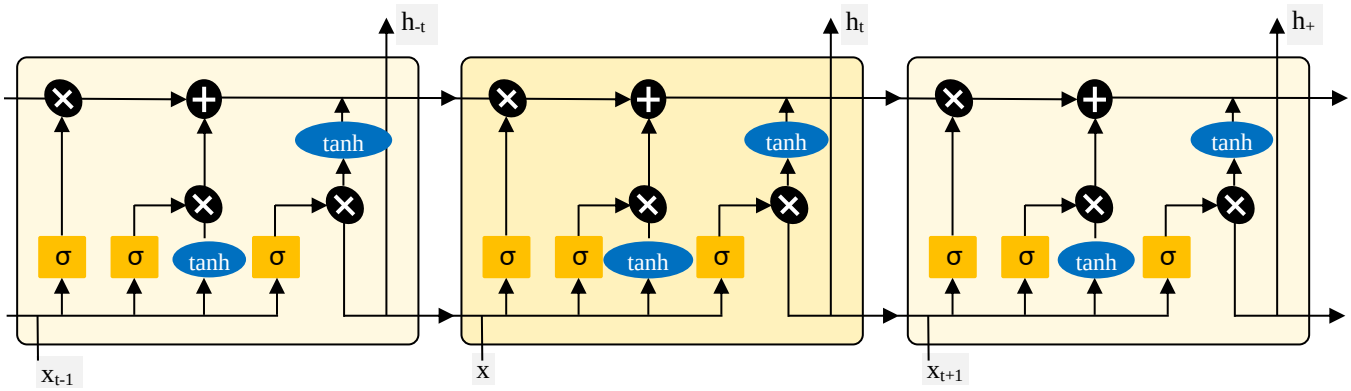

Fig. 3 LSTM architecture

Table 1. Deails of dataset

Classes	Samples Numbers
Early Blight	5500
Late Blight	10450
Leaf Mold	5225
Target Spot	7700
Healthy	8250
Total Samples	**37125**

Fig. 4 Sample images

4. Experimental Validation

In this section, the ISMODL-TLDR approach's tomato leaf ailment recognition achievement is investigated using a dataset, as illustrated in Table 1. Figure 4 signifies the instance images. Figure 5 demonstrates the confusion matrices the ISMODL-TLDR approach gives under 80:20 and 70:30 of TR/TS. The investigational outputs portrayed the efficient detection under overall classes.

Table 2 and Figure 6 depicts the tomato leaf disease recognition outputs of the ISMODL-TLDR approach at 80:20 in the TR/TS. The investigational outputs signified that the ISMODL-TLDR approach recognizes under five classes. On 80% TR, the ISMODL-TLDR approach offers average $accu_y$, $prec_n$, $reca_l$, F_{score}, and AUC_{score} values of 95.07%, 87.35%, 87.06%, 87.19%, and 91.97% correspondingly.

Similarly, with 20% of TS, the ISMODL-TLDR approach provides an average $accu_y$, $prec_n$, $reca_l$, F_{score}, and AUC_{score} values of 94.90%, 87.13%, 86.42%, 86.71%, and 91.60%, respectively.

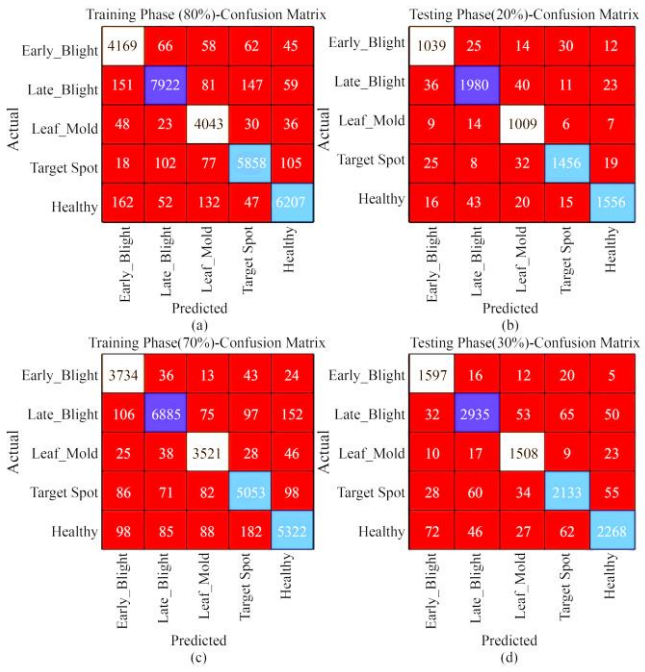

Fig. 5 Confusion matrices of (a-c) 80:70 and (b-d) 20:30 TR/TS phase

Table 2. Tomato leaf disease detection output of ISMODL-TLDR technique on 80:20 of TR/TS phase

Class	$Accu_y$	$Prec_n$	$Reca_l$	F_{score}	AUC_{score}
TR Phase (80%)					
Early Blight	94.76	82.43	82.13	82.28	89.54
Late Blight	94.76	91.09	90.31	90.70	93.41
Leaf Mold	96.72	89.96	86.00	87.93	92.23
Target Spot	95.09	87.59	88.92	88.25	92.81
Healthy	94.04	85.67	87.95	86.79	91.86
Average	**95.07**	**87.35**	**87.06**	**87.19**	**91.97**
TS Phase (20%)					
Early Blight	94.44	81.73	80.50	81.11	88.68
Late Blight	94.74	90.13	90.86	90.50	93.54
Leaf Mold	96.52	92.27	83.50	87.66	91.14
Target Spot	94.52	84.39	90.39	87.29	93.00
Healthy	94.30	87.16	86.87	87.02	91.63
Average	**94.90**	**87.13**	**86.42**	**86.71**	**91.60**

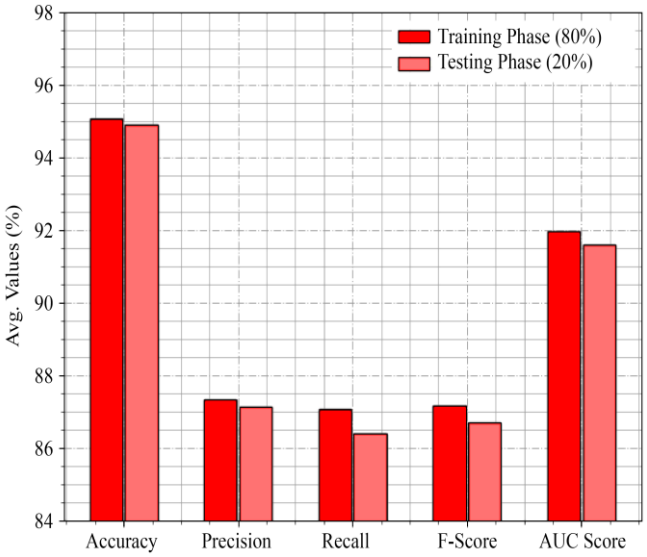

Fig. 6 Average of ISMODL-TLDR technique at 80:20 of TR/TS phase

Table 3. Tomato leaf disease detection outcome of ISMODL-TLDR technique at 70:30 of TR/TS phase

Class	$Accu_y$	$Prec_n$	$Reca_l$	F_{score}	AUC_{score}
TR Phase (70%)					
Early Blight	96.99	89.32	90.83	90.07	94.46
Late Blight	94.12	87.13	92.88	89.91	93.74
Leaf Mold	96.25	95.04	77.51	85.38	88.42
Target Spot	93.74	83.88	85.62	84.74	90.71
Healthy	92.15	82.33	82.56	82.44	88.73
Average	**94.65**	**87.54**	**85.88**	**86.51**	**91.21**
TS Phase (30%)					
Early Blight	96.79	85.99	92.78	89.26	95.12
Late Blight	93.63	86.60	91.34	88.91	92.93
Leaf Mold	96.25	92.95	79.15	85.50	89.09
Target Spot	92.35	83.37	80.91	82.12	88.21
Healthy	91.65	80.94	81.12	81.03	87.87
Average	**94.13**	**85.97**	**85.06**	**85.36**	**90.65**

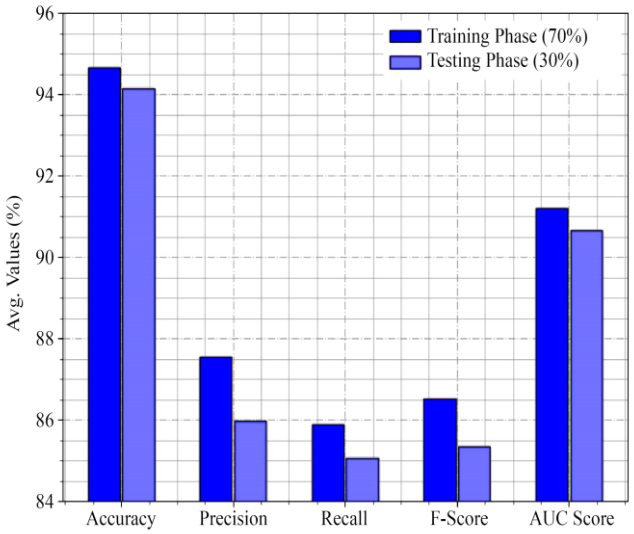

Fig. 7 Average of ISMODL-TLDR technique at 70:30 of TR/TS phase

Table 3 and Figure 7 illustrates the tomato leaf disease detection analysis of the ISMODL-TLDR methodology at 70:30 of TR/TS. The investigational value indicated that the ISMODL-TLDR methodology recognizes under five classes. On 70% of TR, the ISMODL-TLDR methodology portrayed an average $accu_y$, $prec_n$, $reca_l$, F_{score}, and AUC_{score} values of 94.65%, 87.54%, 85.88%, 86.51%, and 91.21% individually. Also, with 20% of the TS Phase, the ISMODL-TLDR methodology exhibited an average $accu_y$, $prec_n$, $reca_l$, F_{score}, and AUC_{score} values of 94.13%, 85.97%, 85.06%, 85.36%, and 90.65% correspondingly. The $accu_y$ curves of the ISMODL-TLDR technique under 80:20 of TR/TS is demonstrated in Figure 8. The figure presents meaningful data concerning the learning tasks and generalization capacities of the BESO-HDLBD method. As epoch counting rises, the TR/TS $accu_y$ curves improve. The ISMODL-TLDR methodology achieves greater testing accuracy that can detect the TR/TS data patterns.

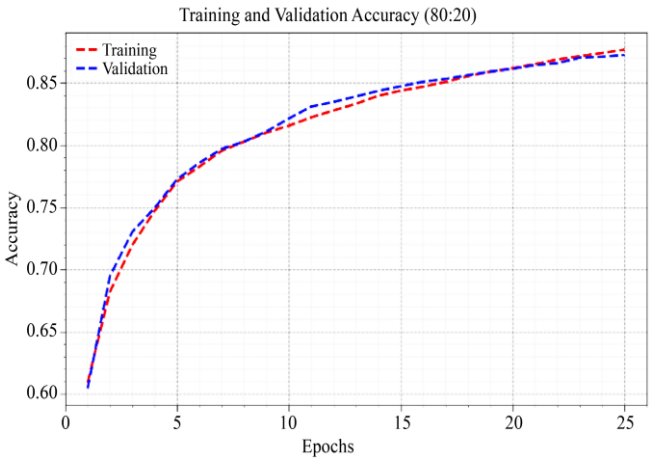

Fig. 8 $Accu_y$ curve of ISMODL-TLDR technique at 80:20 of TR/TS phase

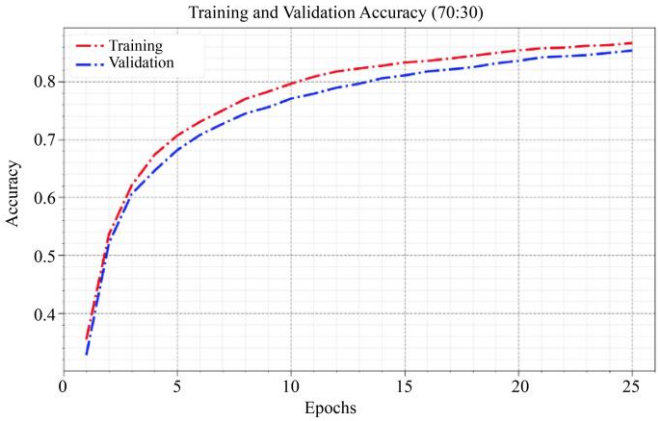

Fig. 9 $Accu_y$ curve of ISMODL-TLDR technique at 70:30 of TR/TS phase

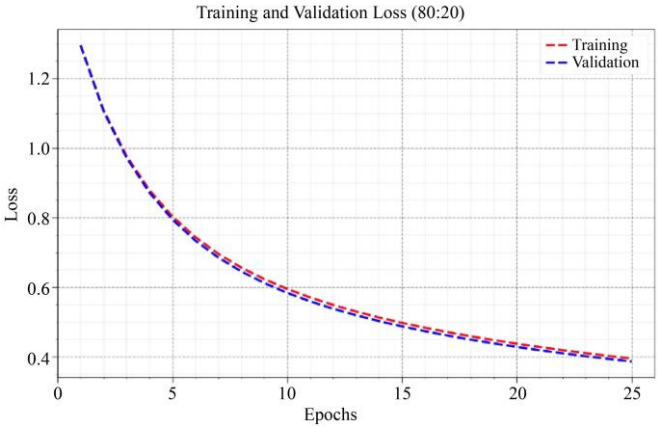

Fig. 10 Loss curve of ISMODL-TLDR technique at 80:20 of TR/TS phase

The $accu_y$ curves of the ISMODL-TLDR technique under 70:30 of TR/TS is shown in Figure 9. The figure presents meaningful data on the learning tasks and generalization abilities of the BESO-HDLBD method. As epoch counting rises, the TR/TS $accu_y$ curves improve. The ISMODL-TLDR methodology achieves greater testing accuracy that can detect the TR/TS data patterns.

Figure 10 illustrates the overall loss of the ISMODL-TLDR method in 80:20 of TR/TS. The loss of TR signifies that the method obtains lessened values, mainly when the process alters the weight to mitigate the anticipation error on TR/TS. The curve of loss indicates the level, in which the method fits the TR data. The loss of TR/TS slowly lessened, exhibiting that the ISMODL-TLDR approach efficaciously captures the patterns specified in TR/TS. The ISMODL-TLDR technique alters the parameters to mitigate variances between the actual and anticipated TR classes. The overall loss of the ISMODL-TLDR method in 70:30 of TR/TS is depicted in Fig. 11. The reduction in TR loss shows that the model is altering weights to reduce prediction errors on TR/TS. The loss curve indicates how well the method fits the TR data. A gradual decrease in TR/TS loss suggests that the ISMODL-TLDR approach effectively captures patterns in TR/TS, with the technique adjusting parameters to reduce discrepancies between actual and predicted TR classes.

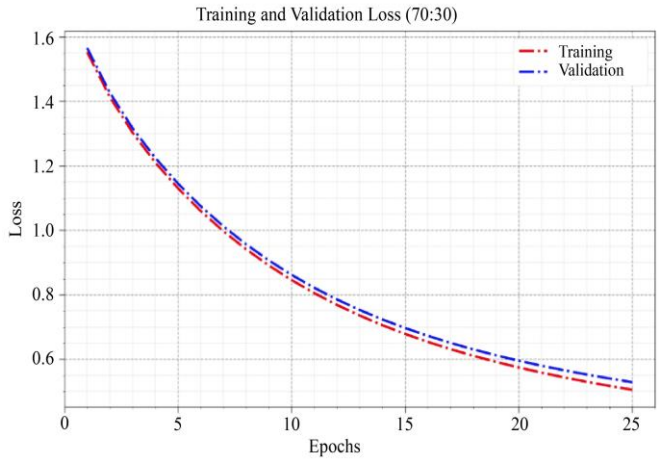

Fig. 11 Loss curve of ISMODL-TLDR technique at 70:30 of TR/TS phase

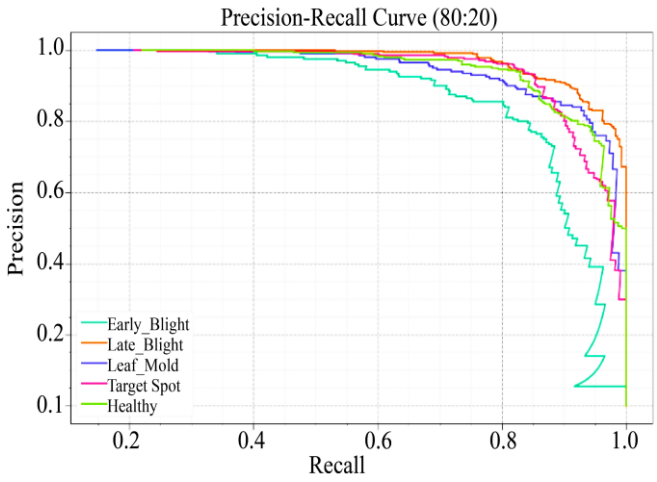

Fig. 12 PR curve of ISMODL-TLDR technique at 80:20 of TR/TS phase

The PR evaluation of the ISMODL-TLDR method under 80:20 of TR/TS is portrayed by plotting $prec_n$ with $reca_l$ as illustrated in Figure 12. The output authorizes that the ISMODL-TLDR method increased values of PR under every 5 class. The figure signifies that the technique learned for detecting various classes. The ISMODL-TLDR technique gets enhanced investigational analysis in identifying positive instances with diminishing false positives.Figure 13 illustrates the PR evaluation of the ISMODL-TLDR method under 70:30 of TR/TS by plotting $prec_n$ with $reca_l$. The output shows that the ISMODL-TLDR method enhanced PR values for every 5 classes. The figure indicates that the technique efficiently learned to detect several classes, with enhanced capability to detect positive instances while reducing false positives.

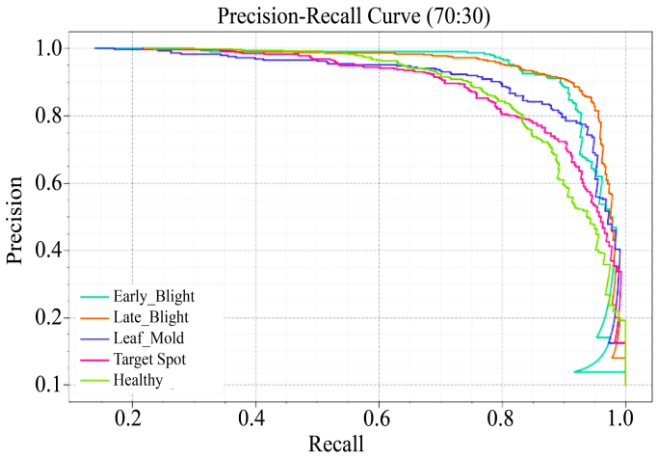

Fig. 13 PR curve of ISMODL-TLDR technique at 70:30 of TR/TS phase

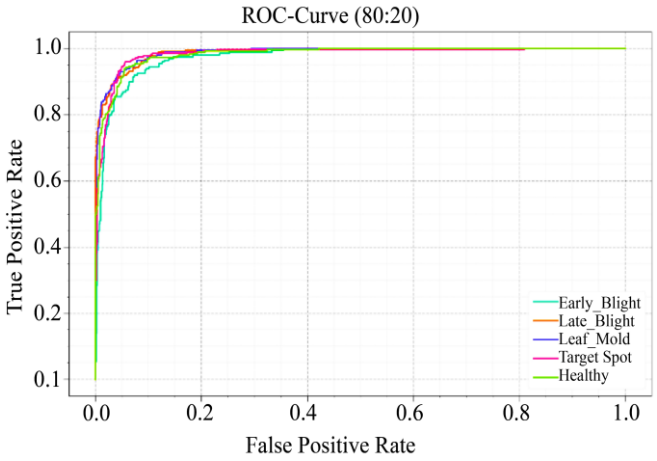

Fig. 14 ROC curve of ISMODL-TLDR technique at 80:20 of TR/TS phase

Figure 14 depicts the ROC evaluation provided by the ISMODL-TLDR methodology under 80:20 of TR/TS, which has the capacity of the class variance.

The figure detects the trade-off amid the rates of TPR/FPR over several classifying thresholds and altering epochs. It portrays the precise anticipation achievement of the ISMODL-TLDR approach in classifying several classes.

The ROC evaluation provided by the ISMODL-TLDR methodology under 70:30 of TR/TS is specified in Figure 15, which has the ability of the class variance. The figure illustrates the trade-off between TPR and FPR across several classification thresholds and epochs. It also accentuates the ISMODL-TLDR approach's performance in precisely classifying multiple classes.

Table 4 and Figure 16 show a relative output of the ISMODL-TLDR technique with the existing model. The investigational outputs stated that the Mobilenet technique achieves the worst outputs. Also, the Vgg16 and Googlenet models have stated slightly increased outcomes.

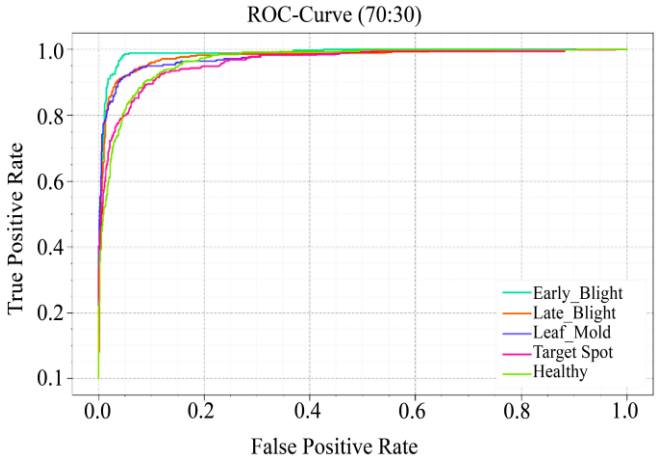

Fig. 15 ROC curve of ISMODL-TLDR technique at 70:30 of TR/TS phase

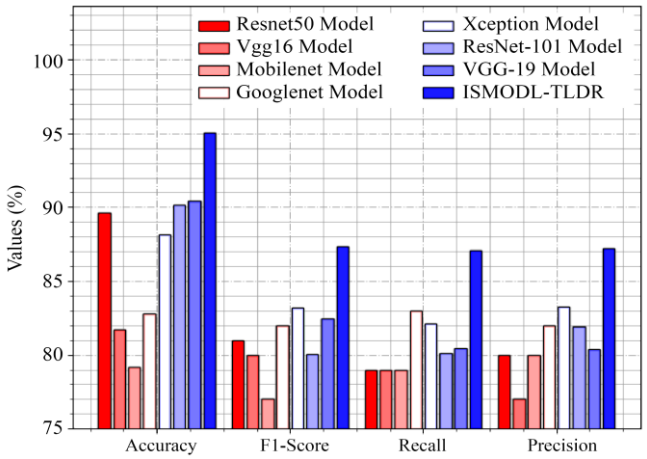

Fig. 16 Comparative output of ISMODL-TLDR technique with other models

Table 4. The comparative output of the ISMODL-TLDR technique with other models

Method	$Accu_y$	$F1_{score}$	$Reca_l$	$Prec_n$
Resnet50	89.65	81.00	79.00	80.00
Vgg16	81.75	80.00	79.00	77.00
Mobilenet	79.20	77.00	79.00	80.00
Googlenet	82.81	82.00	83.00	82.00
Xception	88.16	83.19	82.14	83.25
ResNet-101	90.13	80.04	80.13	81.95
VGG-19	90.42	82.43	80.47	80.39
ISMODL-TLDR	95.07	87.35	87.06	87.19

In the meantime, the Resnet50, Xception, and ResNet-101 techniques accomplish reasonable performance. Although the VGG-19 technique attains significant achievement, the ISMODL-TLDR technique portrays dominance over other methods with maximal $accu_y$ of 95.07%, $F1_{score}$ of 87.35%, $reca_l$ of 87.06%, and $prec_n$ of 87.19%. Thus, the ISMODL-TLDR method can be implemented for tomato leaf disease recognition.

5. Conclusion

In this study, an automated tomato leaf disease detection and classification approach called the ISMODL-TLDR technique is proposed. The ISMODL-TLDR technique incorporates the DL models with a hyperparameter tuning model for tomato leaf disease recognition. It involves several phases of operations, namely WF-based preprocessing, EfficientNet feature extractor, ISMO-based hyperparameter tuning, and LSTM classification. The simulation analysis portrays the enhanced performance of the ISMODL-TLDR technique in terms of classification accuracy. The ISMODL-TLDR technique holds great promise for sustainable agriculture practices, helping farmers make informed decisions and mitigate disease-related crop losses.

References

[1] Sami Ur Rahman et al., "Image Processing Based System for the Detection, Identification and Treatment of Tomato Leaf Diseases," *Multimedia Tools and Applications*, vol. 82, no. 6, pp. 9431-9445, 2023. [CrossRef] [Google Scholar] [Publisher Link]

[2] C. Senthilkumar, and M. Kamarasan, "An Effective Citrus Disease Detection and Classification Using Deep Learning Based Inception Resnet V2 Model," *Turkish Journal of Computer and Mathematics Education*, vol. 12, no. 12, pp. 2283-2296, 2021. [CrossRef] [Google Scholar] [Publisher Link]

[3] U. Shruthi et al., "Tomato Plant Disease Classification Using Deep Learning Architectures: A Review," *Proceedings of Second International Conference on Advances in Computer Engineering and Communication Systems: ICACECS 2022*, pp. 153-169, 2022. [CrossRef] [Google Scholar] [Publisher Link]

[4] Vishal Seth, Rajeev Paulus, and Anil Kumar, *Tomato Leaf Diseases Detection Using Deep Learning-A Review*, Intelligent Systems and Smart Infrastructure, CRC Press, 1st ed., 2023. [Google Scholar] [Publisher Link]

[5] Rishabh Mudgil et al., "Identification of Tomato Plant Diseases Using CNN-A Comparative Review," *2022 IEEE World Conference on Applied Intelligence and Computing (AIC)*, Sonbhadra, India, pp. 174-181, 2022. [CrossRef] [Google Scholar] [Publisher Link]

[6] Yaser AbdulAali Jasim, "High-Performance Deep learning to Detection and Tracking Tomato Plant Leaf Predict Disease and Expert Systems," *ADCAIJ: Advances in Distributed Computing and Artificial Intelligence Journal*, vol. 10, no. 2, 2021. [CrossRef] [Google Scholar] [Publisher Link]

[7] Reesali Mohanty et al., "Tomato Plant Leaves Disease Detection Using Machine Learning," *2022 International Conference on Applied Artificial Intelligence and Computing (ICAAIC)* Salem, India, pp. 544-549, 2022. [CrossRef] [Google Scholar] [Publisher Link]

[8] Sanjeela Sagar, and Jaswinder Singh, "An Experimental Study of Tomato Viral Leaf Diseases Detection Using Machine Learning Classification Techniques," *Bulletin of Electrical Engineering and Informatics*, vol. 12, no. 1, pp. 451-461, 2023. [CrossRef] [Google Scholar] [Publisher Link]

[9] M.T. Vasumathi, and M. Kamarasan, "An Effective Pomegranate Fruit Classification Based on CNN-LSTM Deep Learning Models," *Indian Journal of Science and Technology*, vol. 14, no. 16, pp. 1310-1319, 2021. [CrossRef] [Google Scholar] [Publisher Link]

[10] N. Aishwarya et al., "Smart Farming for Detection and Identification of Tomato Plant Diseases Using Light Weight Deep Neural Network," *Multimedia Tools and Applications*, vol. 82, no. 12, pp. 18799-18810, 2023. [CrossRef] [Google Scholar] [Publisher Link]

[11] Amreen Abbas et al., "Tomato Plant Disease Detection Using Transfer Learning with C-GAN Synthetic Images," *Computers and Electronics in Agriculture*, vol. 187, 2021. [CrossRef] [Google Scholar] [Publisher Link]

[12] Kyamelia Roy et al., "Detection of Tomato Leaf Diseases for Agro-Based Industries Using Novel PCA DeepNet," *IEEE Access*, vol. 11, pp. 14983-15001, 2023. [CrossRef] [Google Scholar] [Publisher Link]

[13] Mariam Moussafir et al., "Design of Efficient Techniques for Tomato Leaf Disease Detection Using Genetic Algorithm-Based and Deep Neural Networks," *Plant and Soil*, vol. 479, no. 1-2, pp. 251-266, 2022. [CrossRef] [Google Scholar] [Publisher Link]

[14] Changjian Zhou et al., "Tomato Leaf Disease Identification by Restructured Deep Residual Dense Network," *IEEE Access*, vol. 9, pp. 28822-28831, 2021. [CrossRef] [Google Scholar] [Publisher Link]

[15] Antonio Guerrero-Ibañez, and Angelica Reyes-Muñoz, "Monitoring Tomato Leaf Disease through Convolutional Neural Networks," *Electronics*, vol. 12, no. 1, pp. 1-15, 2023. [CrossRef] [Google Scholar] [Publisher Link]

[16] Hareem Kibriya et al., "Tomato Leaf Disease Detection Using Convolution Neural Network," *2021 International Bhurban Conference on Applied Sciences and Technologies (IBCAST)*, Islamabad, Pakistan, pp. 346-351, 2021. [CrossRef] [Google Scholar] [Publisher Link]

[17] T. Anandhakrishnan, and S.M. Jaisakthi, "Deep Convolutional Neural Networks for Image Based Tomato Leaf Disease Detection," *Sustainable Chemistry and Pharmacy*, vol. 30, 2022. [CrossRef] [Google Scholar] [Publisher Link]

[18] K. Mahadevan, A. Punitha, and J. Suresh, "A Novel Rice Plant Leaf Diseases Detection Using Deep Spectral Generative Adversarial Neural Network," *International Journal of Cognitive Computing in Engineering*, vol. 5, pp. 237-249, 2024. [CrossRef] [Google Scholar] [Publisher Link]

[19] Chunguang Bi et al., "Optimizing a Multi-Layer Perceptron Based on an Improved Gray Wolf Algorithm to Identify Plant Diseases," *Mathematics*, vol. 11, no. 15, pp. 1-36, 2023. [CrossRef] [Google Scholar] [Publisher Link]

[20] Ila Kaushik, Nupur Prakash, and Anurag Jain, "Plant Disease Detection Using a Depth-Wise Separable-Based Adaptive Deep Neural Network," *Multimedia Tools and Applications*, pp. 1-29, 2024. [CrossRef] [Google Scholar] [Publisher Link]

[21] Hui-Wen Xie et al., "Improved Ultrasound Image Quality with Pixel-Based Beamforming Using a Wiener-Filter and a SNR-Dependent Coherence Factor," *Ultrasonics*, vol. 119, 2022. [CrossRef] [Google Scholar] [Publisher Link]

[22] Mingxing Tan, and Quoc Le, "EfficientNet: Rethinking Model Scaling for Convolutional Neural Networks," *Proceedings of the 36th International Conference on Machine Learning, PMLR*, vol. 97, pp. 6105-6114, 2019. [Google Scholar] [Publisher Link]

[23] Jinhao Du, Jabir Mumtaz, and Jingyan Zhong, "Improved Spider Monkey Optimization Algorithm for Hybrid Flow Shop Scheduling Problem with Lot Streaming," *Engineering Proceedings*, vol. 45, no. 1, pp. 1-4, 2023. [CrossRef] [Google Scholar] [Publisher Link]

[24] Pengtao Li et al., "A Hybrid Deep Learning Model for Short-Term PV Power Forecasting," *Applied Energy*, vol. 259, 2020. [CrossRef] [Google Scholar] [Publisher Link]